J Inf Process Syst, Vol.13, No.2, pp.305~320, April 2017
https://doi.org/10.3745/JIPS.02.0056

ISSN 1976-913X (Print)
ISSN 2092-805X (Electronic)

JOURNAL OF INFORMATION PROCESSING SYSTEMS JIPS

Self-adaptive and Bidirectional Dynamic Subset Selection Algorithm for Digital Image Correlation

Wenzhuo Zhang*, Rong Zhou*, and Yuanwen Zou*

Abstract

The selection of subset size is of great importance to the accuracy of digital image correlation (DIC). In the traditional DIC, a constant subset size is used for computing the entire image, which overlooks the differences among local speckle patterns of the image. Besides, it is very laborious to find the optimal global subset size of a speckle image. In this paper, a self-adaptive and bidirectional dynamic subset selection (SBDSS) algorithm is proposed to make the subset sizes vary according to their local speckle patterns, which ensures that every subset size is suitable and optimal. The sum of subset intensity variation (η) is defined as the assessment criterion to quantify the subset information. Both the threshold and initial guess of subset size in the SBDSS algorithm are self-adaptive to different images. To analyze the performance of the proposed algorithm, both numerical and laboratory experiments were performed. In the numerical experiments, images with different speckle distribution, different deformation and noise were calculated by both the traditional DIC and the proposed algorithm. The results demonstrate that the proposed algorithm achieves higher accuracy than the traditional DIC. Laboratory experiments performed on a substrate also demonstrate that the proposed algorithm is effective in selecting appropriate subset size for each point.

Keywords

Digital Image Correlation, Dynamic Subset Size, Image Processing, Information Amount, Self-adaptive

1. Introduction

Digital image correlation (DIC) is a contactless technique able to measure full-field deformation. Since it was first proposed in the 1980s [1,2], the DIC method has been the most popular and widely used measuring technique due to its many advantages, such as fewer requirements in experimental environment, wide application scope and its high accuracy [3-5].

The principle of DIC is to search the optimal match between the reference subset in the undeformed image and the corresponding target subset in the deformed image by mathematically locating their optimal similarity [6]. In the DIC method, the subset is the matching unit, so it is obvious that the selection of subset size would seriously impact the accuracy and reliability of DIC [7]. On the one hand, the subset should be large enough to contain sufficient speckles or intensity variations to ensure its unique and accurate identification in the deformed image. The use of small subset may result in relatively bigger random errors due to the mismatch of subsets. On the other hand, subset should be as

Manuscript received January 24, 2017; first revision February 8, 2017; accepted March 4, 2017.
Corresponding Author: Yuanwen Zou (zyw@scu.edu.cn)
* College of Materials Science and Engineering, Sichuan University, Chengdu, China (mzhangwz@126.com, buaazhourong@163.com, zyw@scu.edu.cn)

small as possible to guarantee that the actual deformation can be correctly approximated by the predefined shape function in DIC. The use of large subset may cause relatively bigger systematic errors due to incorrect approximation of the shape function. Thus, the selection of subset size is a trade-off between random errors and systematic errors, and is undoubtedly an important but confusing problem to the users of DIC. In practice, several different subset sizes need to be tested systematically in the DIC process for acquiring the optimal one, which would be very time-consuming and very inefficient.

It is observed that the selection of subset size depends on the quality of speckle patterns around the calculation points [8-14]. Several different assessment parameters of speckle patterns have been proposed during the past few years, such as the speckle size [9], the subset entropy [10], the sum of square of subset intensity gradient (SSSIG) [11], the mean intensity gradient (MIG) [12] and the Shannon entropy [13]. However, most of these parameters, no matter whether they are global or local parameters, are aimed at looking for an optimal global subset size and applying it to the whole image throughout the DIC analysis. Nevertheless, a same subset size may not be appropriate to deal with the whole image as the speckle distribution might be inconsistent in different regions. A fixed subset size is too large for the regions with dense speckle distribution, whereas it may be too small for the sparse areas. It is clearly preferable to apply a dynamic subset selection algorithm, in which the subset sizes can vary according to their local speckle patterns.

Hassan et al. [15] proposed a dynamic subset selection (DSS) algorithm to vary the subset sizes via using the intensity variation ratio (Λ) as the assessment criterion. Λ is the ratio of the length of pattern edges within a subset to the perimeter of the subset. This algorithm is effective to the images with uniform speckle distribution, but may not be appropriate to the non-uniform situation, because in the latter situation, the ratio Λ does not show a corresponding change as subset size changes. When the subset size increases, both the perimeter of the subset and the length of pattern edges would potentially increase, which may result in the unexpected decrease of Λ. It should be noted that Λ does not seem to perform well in terms of assessing whether a subset has sufficient information. In addition, a particular value of Λ, obtained from a series of experiments, is recommended as the threshold in the dynamic process. However, this particular value is not self-adaptive and may not be suitable for all images, because the recommended particular value does not consider the differences of actual speckle patterns in different images. When this value is not appropriate, it is also very time-consuming to repeat the numerous experiments to find another appropriate threshold.

A good dynamic subset size selection algorithm should be adaptive to different images and should be able to select the optimal subset size at each calculation point. In this paper, a self-adaptive and bidirectional dynamic subset selection (SBDSS) algorithm is proposed to meet these requirements. In the SBDSS algorithm, the information amount threshold and the initial guess of subset size are self-adaptive to different images on the basis of their speckle pattern qualities and could be calculated automatically. The optimal subset size at each point can be dynamically selected based on its local speckle pattern, ensuring each subset contains sufficient but not redundant information amount, which would improve the accuracy of DIC.

2. Outline of Digital Image Correlation

DIC is an optical-numerical full-field measuring technique. In its basic principle, the displacement

field is calculated by matching the same points between the reference image and the deformed image, recorded before and after deformation, respectively. Before the calculation of the displacements in DIC, a region of interest (ROI) should be specified in the reference image, in which the calculation points are further generated by mesh division. Subsequently, a calculation-point-centered square subset of (2*M*+1) × (2*M*+1) pixels is chosen as the matching unit, and then used to track or match its corresponding location in the deformed image [3], as schematically illustrated in Fig. 1.

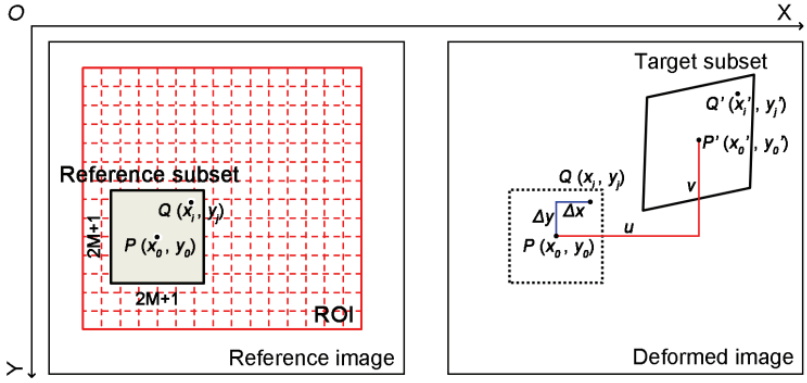

Fig. 1. Subsets in the reference image and the deformed image.

As shown in Fig. 1, both the location and the shape of the reference subset are changed. DIC is based on the assumption of deformation continuity that the neighboring points in a reference subset remain neighboring in the target subset. Thus, the shape function can be used to approximate the actual deformation. The shape function includes the zero-order shape function, the first-order shape function, the second-order shape function and so on. The first-order shape function allows translation, rotation, shear, normal strains and their combinations of the subset and is now most commonly used [3]. In this paper, the first-order shape function is used, which is presented mathematically as:

$$x_i' = x_i + u + u_x \Delta x + u_y \Delta y \tag{1}$$

$$y_j' = y_j + v + v_x \Delta x + v_y \Delta y \tag{2}$$

where (x_i, y_j) denote the coordinates in the reference image, (x_i', y_j') denote the corresponding coordinates in the deformed image, u, v are the x- and y-directional displacement components of the subset center ($P(x_0, y_0)$, Fig. 1), u_x, u_y, v_x, v_y are the first-order displacement gradients of the reference subset, Δx , Δy are the coordinate distances from other points ($Q(x_i, y_j)$, Fig. 1) in the reference subset to the subset center.

It can be observed from Eqs. (1) and (2) that, the coordinates of point (x_i', y_j') in the deformed image may locate between pixels (sub-pixel location). Thus, a certain sub-pixel interpolation scheme should be utilized. In this study, the forth-order keys interpolation algorithm [16] is used owing to its small bias errors and negligible rotation errors.

To evaluate the similarity between the reference subset and its deformed counterpart, a certain correlation criterion must be defined in advance. In this study, the zero-normalized sum of squared differences (C_{ZNSSD}) parameter is chosen as the correlation criterion. C_{ZNSSD} offers robust noise-proof

performance and is insensitive to the offset and linear scale in illumination lighting [17]:

$$C_{\mathrm{ZNSSD}} = \sum_{i=-M}^{M}\sum_{j=-M}^{M}\left[\frac{f(x_i,y_j)-f_m}{\sqrt{\sum_{i=-M}^{M}\sum_{j=-M}^{M}\left[f(x_i,y_j)-f_m\right]^2}} - \frac{g\left(x_i',y_j'\right)-g_m}{\sqrt{\sum_{i=-M}^{M}\sum_{j=-M}^{M}\left[g\left(x_i',y_j'\right)-g_m\right]^2}}\right]^2 \quad (3)$$

where $f(x_i, y_j)$ is the gray level intensity at coordinates (x_i, y_j) in the reference subset of the reference image, $g(x_i', y_j')$ is the gray level intensity at coordinates (x_i', y_j') in the target subset of the deformed image, f_m, g_m are the mean intensity values of the reference subset and the target subset, respectively. The size of the subset in Eq. (3) is $(2M+1) \times (2M+1)$ pixels.

Substituting Eqs. (1) and (2) into Eq. (3), the correlation function would become a nonlinear function with respect to the desired displacement vector $\mathbf{P} = (u, v, u_x, u_y, v_x, v_y)^T$. In order to speed up the acquiring process of the desired displacement vector, various algorithms have been proposed in literatures [3]. In this study, the commonly used Newton-Raphson algorithm [18,19] is utilized because of its high accuracy.

As shown in Eq. (3), the parameter M relative to the subset size plays an important role in the correlation calculation. The subset should be large enough to contain a sufficiently distinctive intensity pattern to guarantee its correct match. However, the subset should also be small enough to ensure that its actual deformation can be correctly approximated by the first-order shape function, shown in Eqs. (1) and (2). Therefore, the selection of subset size should be a trade-off. In addition, the speckle patterns naturally occurring or artificially prepared often present distinctly different distribution characteristics, such as non-uniform speckle distribution. A fixed subset size cannot perform well on the sparse and the dense speckle distribution regions at the same time. It is preferable to vary subset sizes according to their local speckle patterns. Therefore, the SBDSS algorithm is proposed in this paper.

3. Self-adaptive and Bidirectional Dynamic Subset Selection Algorithm

3.1 Assessment Criterion

In order to achieve the dynamic selection of subset size, a certain criterion able to quantify the information amount within a subset should be defined first. Matching information amount is highly related to the patterns of speckles. Thus, the intensity gradients within a subset can be used to represent or describe its information amount. The intensity gradients include those along x-direction, y-direction and x-y-direction. Yaofeng and Pang [10] proposed the subset entropy on the basis of intensity gradients along all directions. However, the parameter "subset entropy" is an average value, thus this parameter cannot increase with the increase of subset size, meaning that the subset entropy is not a proper dynamic assessment criterion to represent the information amount within a subset. In this paper, a parameter called the sum of subset intensity variation (η) is proposed to quantify the information amount within a subset:

$$\eta = \sum_{P\in S}\sum_{i=1}^{8}|I_P - I_i| \quad (4)$$

where S denotes a subset, P denotes a pixel point in S, I_P is the intensity at P, and I_i is the intensity at one of eight neighboring points of P. η is the sum of intensity gradients within a subset along all directions, including x-direction, y-direction and x-y-direction. η is closely related to the subset size and could increase with the increase of subset size.

3.2 Information Amount Threshold

Every dynamic algorithm needs a stop condition, namely a threshold. In the SBDSS algorithm, the threshold represents the critical point where the subset exactly owns sufficient information amount, which will guarantee the successful matching. In this paper, we call it the threshold sum of subset intensity variation (η_{th}).

Hassan et al. [20] proposed that a subset should contain an average of four or more speckles to achieve high accuracy in DIC. Therefore, the number of speckles could be used to calculate η_{th}. In this paper, N is defined as the number of speckles representing that one subset has sufficient information to be identified. Thus, η_{th} can be defined as the average information amount of N speckles:

$$\eta_{th} = \frac{N}{n}\eta_{ROI} \tag{5}$$

$$n = \frac{1}{4\pi}\frac{(2n\pi r)^2}{n\pi r^2} = \frac{1}{4\pi}\frac{{L_{spk}}^2}{S_{spk}} \tag{6}$$

where η_{ROI} is the η of the whole ROI, it can be computed via Eq. (4) by replacing the parameter S with the ROI, n denotes the total number of speckles in the ROI, and r denotes the average radius of all speckles in the ROI. Most speckles can be considered as circles, thus the area and perimeter equations of circle are used. For some specific speckle patterns, if another shape is more suitable, this method would also be valid, and users only need to change the parameters in Eq. (6). S_{spk} and L_{spk} represent the total area and total edge length of all speckles in the ROI, respectively. There are two steps during the calculation process of S_{spk} and L_{spk}: first, use the Otsu's method [21] to binarize the ROI and further count its speckle pixels, the total number of speckle pixels is the S_{spk}; second, perform edge extraction on the binarized ROI and then count the edge pixels, the total number of the edge pixels is the L_{spk}.

According to the equations mentioned above, η_{th} can be calculated automatically and is self-adaptive to different images, which can be further applied in the SBDSS algorithm as the stop condition.

3.3 Optimized Initial Guess of Subset Size

For a dynamic subset size selection algorithm, it is a waste of time that the initial dynamic subset size at every point increases from a small value until satisfying the condition $\eta>=\eta_{th}$. In this paper, an optimized initial guess of subset size is proposed.

As mentioned above, one subset owning N speckles is assumed to have sufficient information amount. Therefore, the initial guess of subset size can be defined as the average subset size containing N speckles:

$$Size_{init} = \sqrt{\frac{N}{n}WH} \tag{7}$$

where W and H denote the width and height of the ROI, n is the total number of speckles in the ROI which is calculated by Eq. (6). After optimizing the $Size_{init}$, the dynamic subset selection would achieve the bidirectional change of subset size within a small range, which can significantly reduce the dynamic times and improve its efficiency. Because the $Size_{init}$ is a global parameter based on the characteristics of the image, the $Size_{init}$ is also self-adaptive.

3.4 Process of SBDSS Algorithm

The detail process of the SBDSS algorithm is as follows:

- **Step 1:** Define the value of N according to the speckle patterns (the appropriate number of speckles that a subset should have), and further calculate the information amount threshold η_{th} and the initial subset size $Size_{init}$.

- **Step 2:** Dynamically adjust the subset size and find the optimal one. It is the core part of the dynamic subset selection algorithm, and the pseudo code is as follows:

```
1   SubsetSize = Size_init
2   Compute η by SubsetSize
3   If ( η < η_th )
4       Then   IsSmall = TRUE
5       Else   IsSmall = FALSE
6   End if
7   If ( IsSmall == TRUE )
8       Then   increase SubsetSize by a Step and re-compute the η, until η >= η_th
9       Else   decrease SubsetSize by a Step and re-compute the η, until η < η_th
10              SubsetSize = SubsetSize + Step
11  End if
```

As the pseudo code described above, the adjustment of subset size is bidirectional. The change direction of subset size is determined in the 1st until 6th line, and dynamic adjustment is shown in the 7th until 11th line. If $\eta<\eta_{th}$, it means that the information amount within the current subset is not sufficient, thus the subset size needs to increase by a *Step*. If $\eta>\eta_{th}$, it indicates the information amount is sufficient even might be redundant, thus the subset size needs to decrease by a *Step*. For each calculation point, its optimal subset size is the smallest value which satisfy the requirement $\eta>=\eta_{th}$. This subset selection method ensures sufficient information within a subset, and also reduces the subset size as much as possible, which guarantees both random errors and systematic errors in a relatively low level.

Step represents the subset size change step and it can be defined as two or other pixels depending on the image. Besides, it is recommended to set a dynamic range, namely the upper limit and lower limit of subset size.

- **Step 3:** Perform the rest procedure of the DIC analysis by using the subset size obtained from Step 2. Repeat Step 2 and Step 3 point by point in the ROI until all calculation points are computed.

In summary, the SBDSS algorithm can achieve dynamic subset selection according to the local speckle patterns, and ensure that subset size at each point is suitable and optimal. In addition, since the η_{th} and

the $Size_{init}$ are self-adaptive to different images, the SBDSS algorithm can be used to deal with many types of images. By comparing with other dynamic subset selection algorithms, the optimization of the $Size_{init}$ in SBDSS accelerates the process of dynamic subset selection. The SBDSS algorithm extends the application scope of DIC.

4. Experimental Verification

In order to evaluate the performance of the SBDSS algorithm, both numerical experiments and laboratory experiments were conducted.

4.1 Numerical Experiments

To evaluate the accuracy of the SBDSS algorithm, a series of numerical experiments were conducted. Peng and Goodson [22] proposed an approach based on Gaussian speckles to generate speckle images. These images could provide well-controlled image features and deformation information.

$$I_1(\mathbf{r}) = \sum_{k=1}^{s} I_0 \exp\left(-\frac{|\mathbf{r}-\mathbf{r}_k|^2}{a^2}\right) \tag{8}$$

$$I_2(\mathbf{r}) = \sum_{k=1}^{s} I_0 \exp\left(-\frac{|\mathbf{r}-\mathbf{U}(\mathbf{r})-\mathbf{r}_k|^2}{a^2}\right) \tag{9}$$

where I_1 and I_2 denote the reference image and the deformed image, respectively, s is the total number of speckles, a is the speckle size, I_0 is the peak intensity of each speckle, $\mathbf{r}_k = (x_k, y_k)^T$ are the coordinates of speckles with a random distribution. $\mathbf{U}(\mathbf{r})$ is the predefined displacement function.

In numerical experiments, two reference images with 600 × 600 pixels were generated by Eq. (8), one of which is the image with uniform speckle distribution (Image A, Fig. 2(a)), and the other is the image with non-uniform speckle distribution (Image B, Fig. 2(b)), sparse in the middle region and dense in the top and bottom sides.

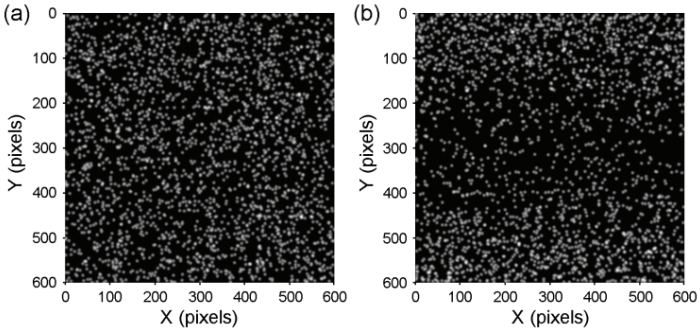

Fig. 2. Numerically generated reference images: (a) Image A with uniform speckle distribution and (b) Image B with non-uniform speckle distribution.

It is generally the case in practical applications where actual displacements are not homogeneous and may not be approximated correctly by any predefined shape function. To take the complex deformation

situation into consideration, nonhomogeneous displacement function [10] was applied to generate deformed images:

$$x' = (1 + \varepsilon)(x - W/2) + W/2 \tag{10}$$

$$y' = y \tag{11}$$

$$\varepsilon = \varepsilon_0[4(y/H - 0.5)^2 - 1] \tag{12}$$

where the intensity at coordinates (x', y') in the generated deformed image equals to that at coordinates (x, y) in the reference image, W and H is the width and height of the image, respectively. ε_0 is the deformation parameter to control the deformation of the image. Fig. 3 shows the deformed image based on Image B at $\varepsilon_0 = 0.1$.

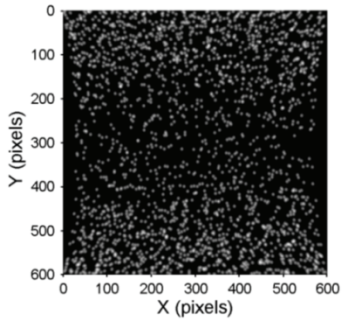

Fig. 3. Numerically generated deformed image based on Image B at $\varepsilon_0 = 0.1$.

It is known that images acquired through cameras might be contaminated by a variety of different noise. Thus, the influence of noise was also investigated in this paper. The noise separately introduced to the intensity of the pixels of the reference images and the deformed images, was random Gaussian noise of a zero mean with standard deviation of 3%. Gaussian noise simulates the acquisition errors resulting from high temperature and poor illumination. All experimental cases are showed in Table 1. According to Table 1, eight pairs of images including the reference images and the deformed images were generated by combining with different speckle distribution, different deformation and noise. Group A is the images with uniform speckle distribution, while Group B represents the images with non-uniform speckle distribution.

Table 1. All experimental cases

	Speckle distribution	ε_0	Noise	Case
Group A	Uniform	0.05	-	1
			Gaussian	2
		0.1	-	3
			Gaussian	4
Group B	Non-uniform	0.05	-	5
			Gaussian	6
		0.1	-	7
			Gaussian	8

In numerical experiments, two different methods including the traditional DIC and the proposed SBDSS algorithm were used to deal with all cases. In the traditional DIC, a fixed subset size was used throughout the whole process. Because the optimal global subset size for each case was unknown to us, a series of subset sizes were employed. To evaluate the effect of speckle number within a subset, different values of N (N = 2, 4, 6, 8, respectively) were set and then used in the SBDSS algorithm.

The ROI of all images was a rectangle region centered at coordinates (300,300), sized 450 × 450 pixels. In the ROI, the calculation points were sampled at every 10 pixels. In total, 2025 points were calculated. By comparing the calculation displacements with the predefined displacement function, the calculation errors would be obtained and further used to evaluate the accuracy of the traditional DIC method and the SBDSS-DIC method.

The displacement field calculated by DIC is made up of displacements along x- and y-directions. The actual x-directional displacements can be computed by the predefined displacement function (Eq. (10)), and the actual y-directional displacements are zero (Eq. (11)). Fig. 4 shows the distribution of x-directional displacements calculated by the SBDSS-DIC method (N = 4, Case 5). Fig. 5 shows the results of subset sizes selected by the SBDSS algorithm (N = 4, Case 5).

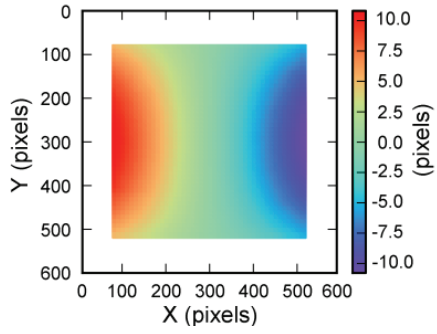

Fig. 4. The distribution of x-directional displacements calculated by SBDSS-DIC (N = 4, Case 5).

It can be seen from Fig. 4 that, the distribution of x-directional displacements is axis-symmetric. The points of both left and right sides move towards the middle of the image. The same displacement value (same color in Fig. 4) appears parabolic distribution along y-direction, which demonstrates that the displacement calculation results agree with the preset displacements in Eq. (10). Fig. 5(a) shows the histogram of subset sizes selected by the proposed SBDSS algorithm. Fig. 5(b) shows the distribution of subset sizes at different calculation points. In Fig. 5(b), the subset sizes located in the top and bottom sides seem smaller (around 30 pixels), while the subset sizes located in the middle region seem larger (around 60 pixels), which is consistent with the speckle distribution characteristics of Image B. Fig. 5 demonstrates the utility of the proposed SBDSS algorithm in dynamically selecting subset sizes.

The displacement of every point contains x- and y-directional components, both of which have errors. To investigate the accuracy of displacement results, the absolute error [15] considering the two directions is used to represent the error at each point:

$$E_a = \sqrt{{E_u}^2 + {E_v}^2} \tag{13}$$

where E_u and E_v are the errors in x- and y-directions, respectively.

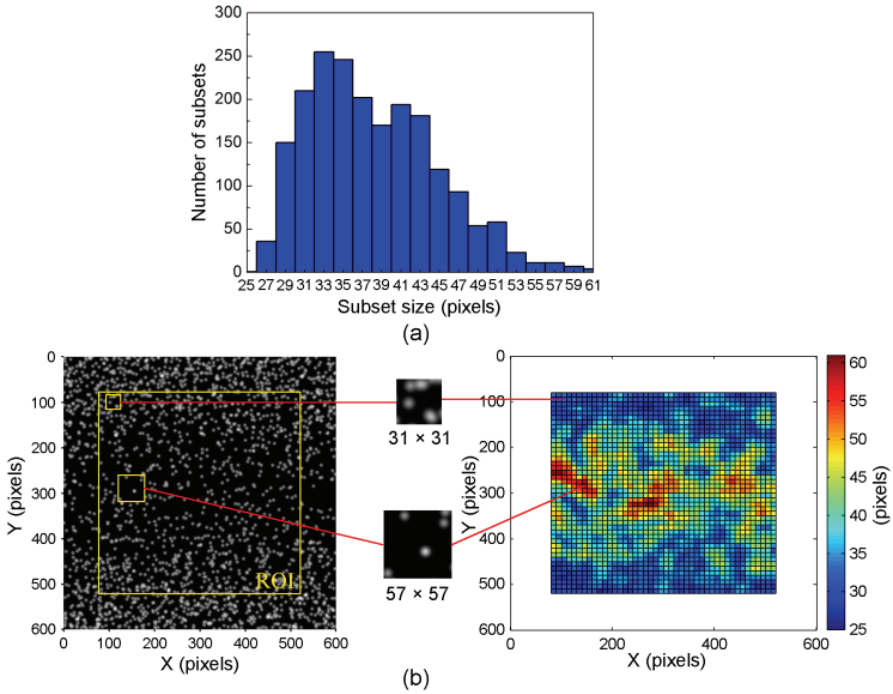

Fig. 5. The results of subset sizes selected by the SBDSS algorithm (N = 4, Case 5): (a) the histogram of subset sizes and (b) the distribution of subset sizes at different calculation points.

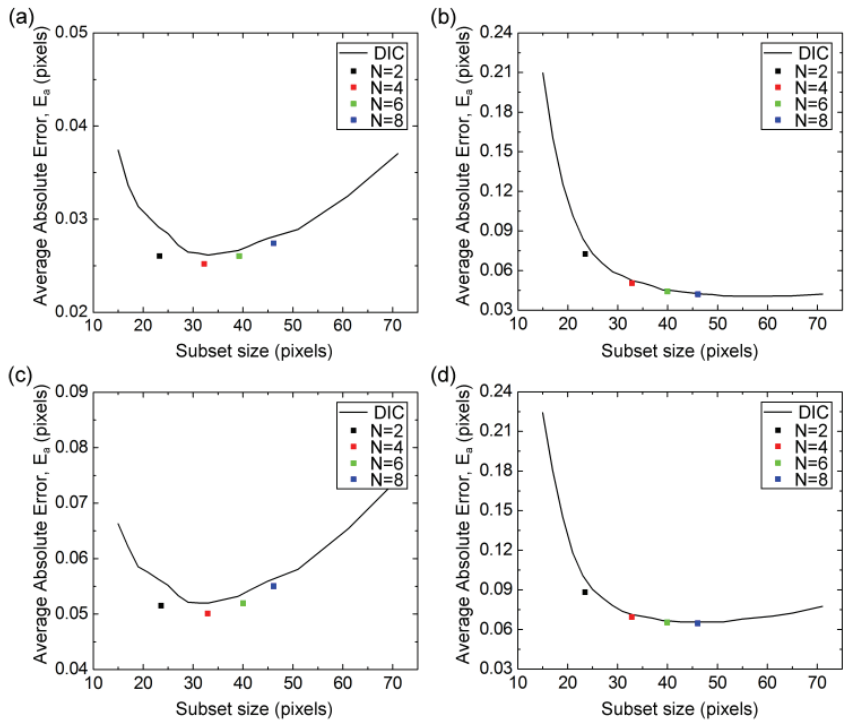

Fig. 6. The error comparison results of Group A; traditional DIC vs. SBDSS-DIC. (a) Case 1, (b) Case 2, (c) Case 3, and (d) Case 4.

Since different calculation points have different E_a, the average value of E_a over the entire ROI is applied to represent the error of a case. Fig. 6 illustrates the error comparison results of Group A (Cases 1 to 4). Fig. 7 illustrates the error comparison results of Group B (Cases 5 to 8). The horizontal axis represents the subset size and the vertical axis represents the average E_a. The solid line is the average E_a by the traditional DIC at different subset sizes. The colorful square is the average E_a by the SBDSS-DIC method at different values of N, and its horizontal coordinate denotes the average subset size after the process of the SBDSS algorithm.

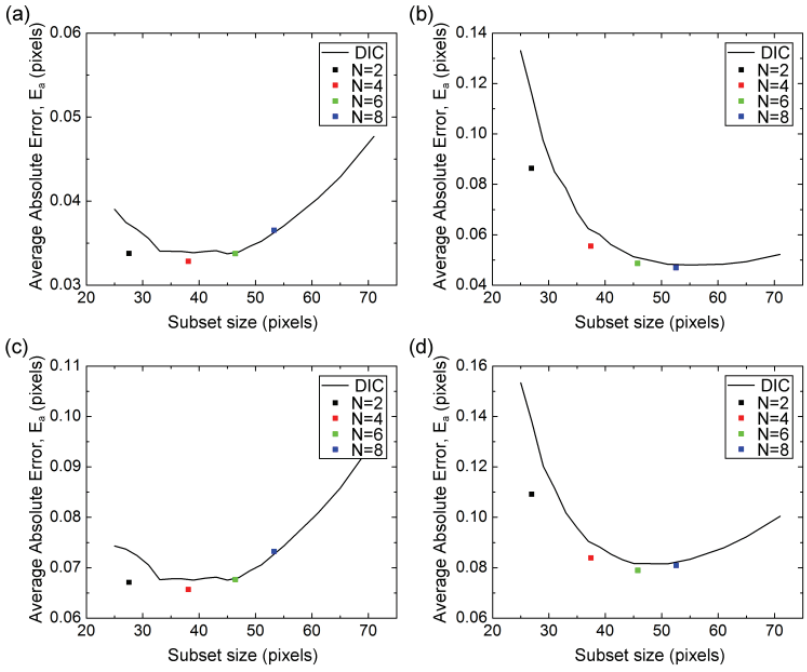

Fig. 7. The error comparison results of Group B; traditional DIC vs. SBDSS-DIC. (a) Case 5, (b) Case 6, (c) Case 7, and (d) Case 8.

It can be seen from Figs. 6 and 7 that, the average E_a of the traditional DIC drops at the initial stage, and then increases after reaching the minimum value when the subset size continues to increase. This agrees with the theoretical analysis that large subset may lead to the relatively larger systematic errors owing to the incorrect approximation of the first-order shape function, whereas small subset would result in bigger random errors due to the mismatch between subsets. The influence of speckle distribution, deformation and noise on the subset selection associated with the accuracy of DIC is discussed as follows.

The images with different speckle distribution include uniform and non-uniform situations, labeled Group A and Group B, respectively. It can be observed by comparing Fig. 6(a) with Fig. 7(a), or Fig. 6(c) with Fig. 7(c) that, the errors of Group A are smaller than the Group B and the curve in Group B is not smooth, the errors of which do not decrease further at the middle subset sizes. In the non-uniform image, the speckle patterns present distinctly different characteristics in different regions so that there does not exist a certain subset size which is optimal for all points. Therefore, the errors of non-uniform images cannot reach to a lowest value at a certain subset size and the curve of errors does not seem

smooth. The optimal global subset size of the traditional DIC in Case 1 (Fig. 6(a)) is 27×27 to 33×33 pixels, while in Case 5 (Fig. 7(a)) it is 33×33 to 47×47 pixels. The results demonstrate that the speckle distribution not only influences the accuracy of DIC but also affects the selection of optimal global subset size.

By comparing the results of different deformation, it can be seen that the average E_a increases with the increase of deformation, but the trend of them is similar with each other. The comparison between Fig. 6(b) and Fig. 6(d), or between Fig. 7(b) and Fig. 7(d) shows that the average E_a in large subset rises more sharply in the cases with larger deformation. Because the first-order shape function cannot correctly approximate the deformation, systematic errors will increase faster when the deformation becomes lager. Thus, different deformation also impacts the accuracy of DIC and the selection of optimal global subset size.

After the introduction of random Gaussian noise, the average E_a in two groups increases noticeably in small subset, but only increases slightly in large subset. Compared with large subset, the small subset is more susceptible. The traditional DIC needs a larger subset size to reduce the impact of random noise. Thus, random noise also affects the accuracy of DIC and the selection of optimal global subset size.

As discussed above, the speckle distribution, deformation and noise will all impact the selection of optimal global subset size and further influence the accuracy of DIC. However, it can be observed from Figs. 6 and 7 that, no matter in what cases, the performance of the proposed SBDSS-DIC method is greater than that of the traditional DIC, even better than the latter at the optimal global subset size. These results indicate that the SBDSS algorithm is more accurate than the traditional DIC.

In the SBDSS algorithm, the value of N is a vital parameter related to the algorithm performance. In this paper, the results of different N can also be seen from Figs. 6 and 7. Without noise (Cases 1, 3, 5, 7), $N = 4$ is optimal, and with noise (Cases 2, 4, 6, 8), $N = 4$, 6, or 8 is optimal, indicating that four speckles contain sufficient information for a subset to be accurately identified. This result agrees with the suggestion of Hassan et al. [20] that, a subset should have average of four or more speckles to achieve high accuracy. Although noise leads to the increase of the optimal value of N, the error differences among $N = 4$, 6, and 8 are slight. Hence, $N = 4$ is recommended in the SBDSS algorithm.

4.2 Laboratory Experiments

To evaluate the utility and the adaptability of the proposed algorithm in practical applications, substrate stretching experiments were performed in this study. Substrate, widely used in cell mechanical experiments, is made up of medical silica gel, which is colorless and transparent. Hence, the speckle patterns need to be artificially prepared. In this study, the speckle patterns were made by spraying black paints on the surface of a substrate specimen. The size of specimen was 140 mm×30 mm (thickness of 0.8 mm).

Fig. 8. Stretch the substrate specimen with both ends clamped.

The apparatus of substrate stretching experiments is shown in Fig. 8. The top and bottom boundaries of the substrate were attached to two clamps. The bottom clamp was fixed to prevent horizontal displacements and rotations, and the top clamp was aligned with the bottom clamp. The load was exerted by a universal material testing machine (AG-IS, SHIMADAZU, Japan) in the vertical direction. All images were captured by a CMOS camera (JHSM1400f, Shenzhen Jinghang Technology Co. Ltd., China), in spatial resolution of 4384×3288 pixels.

The central region of the substrate image with 2200×600 pixels was selected as the ROI in the DIC analysis. The calculation points in the ROI were sampled at every 20 pixels. In total, 3300 points were calculated.

The specimen was loaded vertically. Fig. 9 shows the displacement distribution in the vertical direction calculated by the SBDSS-DIC method (N = 4). As shown in Fig. 9, the displacements change smoothly and uniformly from 6 pixels to 20 pixels along the vertical direction. Fig. 10 shows the histogram of subset sizes selected by the SBDSS algorithm (N = 4). The subset sizes are ranging from 37×37 pixels to 63×63 pixels, which demonstrate that the proposed algorithm is effective in dynamically selecting subset sizes in laboratory experiments.

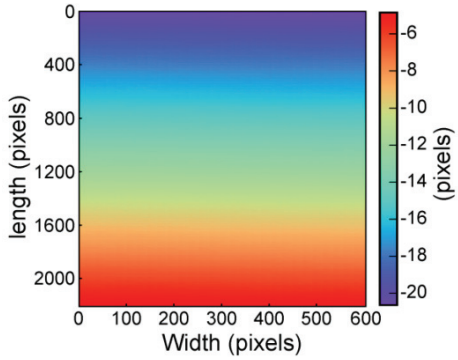

Fig. 9. The displacement distribution in the vertical direction calculated by SBDSS-DIC (N = 4).

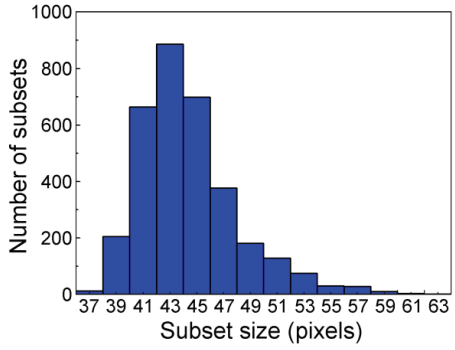

Fig. 10. The histogram of subset sizes selected by the SBDSS algorithm (N = 4).

As mentioned above, the proposed algorithm can calculate correct results and indeed tailor subset sizes according to the local speckle patterns in actual experiments. The specimen in this test was made by spraying black paints, whose speckle patterns are random, and the result of dynamic subset sizes is clear, which verifies the utility and the adaptability of the proposed algorithm. The speckle patterns

naturally occurring often present distinctly different characteristics, so the dynamic effect of our proposed algorithm would be more obvious.

5. Conclusions

In this paper, the SBDSS algorithm which can dynamically select the subset size for each calculation point is proposed. The proposed sum of subset intensity variation (η) is used as the assessment criterion to ensure that every subset size for every point is suitable and optimal, containing sufficient but not redundant information. In addition, both the information amount threshold and the initial guess of subset size in the SBDSS algorithm are self-adaptive to different images and can be calculated automatically.

In order to verify the accuracy and adaptability of the SBDSS algorithm, several numerical and laboratory experiments were performed. The results of the numerical experiments demonstrate that different factors like different speckle distribution, different deformation and noise would affect the selection of optimal global subset size and the proposed algorithm achieves higher accuracy in all test cases than the traditional DIC. The results of the laboratory experiments show the dynamic effect in selecting subset sizes and verify the adaptability of the proposed algorithm. In summary, compared with the traditional DIC, the SBDSS algorithm is consistently more accurate and adaptive for different types of images and eliminates the laborious work in finding the optimal global subset size, which will improve the performance of DIC and expand its application scope.

References

[1] W. H. Peters and W. F. Ranson, "Digital imaging techniques in experimental stress analysis," *Optical Engineering*, vol. 21, no. 3, pp. 427-431, 1982.

[2] T. C. Chu, W. F. Ranson, and M. A. Sutton, "Applications of digital-image-correlation techniques to experimental mechanics," *Experimental Mechanics*, vol. 25, no.3, pp. 232-244, 1985.

[3] B. Pan, K. Qian, H. Xie, and A. Asundi, "Two-dimensional digital image correlation for in-plane displacement and strain measurement: a review," *Measurement Science & Technology*, vol. 20, no. 6, article no. 062001, 2009.

[4] B. Pan, "Recent progress in digital image correlation," *Experimental Mechanics*, vol. 51, no. 7, pp. 1223-1235, 2011.

[5] M. A. Sutton and F. Hild, "Recent advances and perspectives in digital image correlation," *Experimental Mechanics*, vol. 55, no. 1, pp. 1-8, 2015.

[6] S. Yoneyama, "Basic principle of digital image correlation for in-plane displacement and strain measurement," *Advanced Composite Materials*, vol. 25, no. 2, pp. 105-123, 2016.

[7] X. Xu, Y. Su, Y. Cai, T. Cheng, and Q. Zhang, "Effects of various shape functions and subset size in local deformation measurements using DIC," *Experimental Mechanics*, vol. 55, no. 8, pp. 1575-1590, 2015.

[8] D. Lecompte, A. Smits, S. Bossuyt, H. Sol, J. Vantomme, D. V. Hemelrijck, and A. M. Habraken, "Quality assessment of speckle patterns for digital image correlation," *Optics & Lasers in Engineering*, vol. 44, no. 11, pp. 1132-1145, 2006.

[9] T. L. Alexander, J. E. Harvey, and A. R. Weeks, "Average speckle size as a function of intensity threshold level: comparison of experimental measurements with theory," *Applied Optics*, vol. 33, no. 35, pp. 8240-8250, 1994.

[10] S. Yaofeng and J. H. Pang, "Study of optimal subset size in digital image correlation of speckle pattern images," *Optics & Lasers in Engineering*, vol. 45, no. 9, pp. 967-974, 2007.

[11] B. Pan, H. Xie, Z. Wang, K. Qian, and Z. Wang, "Study on subset size selection in digital image correlation for speckle patterns," *Optics Express*, vol. 16, no. 10, pp. 7037-7048, 2008.

[12] B. Pan, Z. Lu, and H. Xie, "Mean intensity gradient: an effective global parameter for quality assessment of the speckle patterns used in digital image correlation," *Optics & Lasers in Engineering*, vol. 48, no. 4, pp. 469-477, 2010.

[13] X. Liu, R. Li, H. Zhao, T. Cheng, G. Cui, Q. Tan, and G. Meng, "Quality assessment of speckle patterns for digital image correlation by Shannon entropy," *Optik - International Journal for Light and Electron Optics*, vol. 126, no. 23, pp. 4206-4211, 2015.

[14] J. Park, S. Yoon, T. H. Kwon, and K. Park, "Assessment of speckle-pattern quality in digital image correlation based on gray intensity and speckle morphology," *Optics & Lasers in Engineering*, vol. 91, pp. 62-72, 2017.

[15] G. M. Hassan, C. MacNish, A. Dyskin, and I. Shufrin, "Digital image correlation with dynamic subset selection," *Optics & Lasers in Engineering*, vol. 84, pp. 1-9, 2016.

[16] R. Keys, "Cubic convolution interpolation for digital image processing," *IEEE Transactions on Acoustics Speech & Signal Processing*, vol. 29, no. 6, pp. 1153-1160, 1981.

[17] B. Pan, H. Xie, and Z. Wang, "Equivalence of digital image correlation criteria for pattern matching," *Applied Optics*, vol. 49, no. 28, pp. 5501-5509, 2010.

[18] H. A. Bruck, S. R. Mcneill, M. A. Sutton, and W. H. Peters, "Digital image correlation using Newton-Raphson method of partial differential correction," *Experimental Mechanics*, vol. 29, no. 3, pp. 261-267, 1989.

[19] G. Vendroux and W. G. Knauss, "Submicron deformation field measurements. Part 2: Improved digital image correlation," *Experimental Mechanics*, vol. 38, no. 2, pp. 86-92, 1998.

[20] G. M. Hassan, A. V. Dyskin, C. K. MacNish, and N. V. Dinh, "A comparative study of techniques of distant reconstruction of displacement and strain fields using the DISTRESS simulator," *Optik - International Journal for Light and Electron Optics*, vol. 127, no. 23, pp. 11288-11305, 2016.

[21] N. Otsu, "A threshold selection method from gray-level histograms," *IEEE Transactions on Systems Man & Cybernetics*, vol. 9, no. 1, pp. 62-66, 1979.

[22] Z. Peng and K. E. Goodson, "Subpixel displacement and deformation gradient measurement using digital image/speckle correlation (DISC)," *Optical Engineering*, vol. 40, no. 8, pp. 1613-1620, 2001.

Wenzhuo Zhang

He received his B.E. degree in Biomedical Engineering from Beihang University, Beijing, China, in 2014. He is currently pursuing his M.E. degree in biomedical information and instrument at Sichuan University, China. His research interests include digital image processing and biomedical information processing.

Rong Zhou

She received her B.E. degree in Biomedical Engineering from Beihang University, Beijing, China, in 2014. She is currently pursuing her M.E. degree in biomedical information and instrument at Sichuan University, China. Her research interests include digital image processing and biomedical device researching.

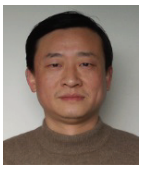

Yuanwen Zou

He is currently a professor at Sichuan University, Chengdu, China. He received his B.E. degree in Automation Engineering from University of Electronic Science and Technology of China in 1989. He received his M.E. degree in Biomedical Engineering from Sichuan University in 1992. He received his Ph.D. degree in Mechanical Engineering and Automation from Sichuan University in 2002. His primary research interests include biomedical signal and information processing, image processing and biomedical device researching.